Deletion of epithelial cell-specific p130Cas impairs the maturation stage of amelogenesis

井上, 茜

Bone 154 (2022) 116210

Contents lists available at ScienceDirect

Bone

journal homepage: www.elsevier.com/locate/bone

Deletion of epithelial cell-specific p130Cas impairs the maturation stage of amelogenesis

Akane Inoue [a,b], Tamotsu Kiyoshima [c], Keigo Yoshizaki [b], Chihiro Nakatomi [d], Mitsushiro Nakatomi [e], Hayato Ohshima [f], Masashi Shin [g,h], Jing Gao [a], Kanji Tsuru [i], Koji Okabe [g], Ichiro Nakamura [j], Hiroaki Honda [k], Miho Matsuda [a], Ichiro Takahashi [b], Eijiro Jimi [a,l,*]

[a] Laboratory of Molecular and Cellular Biochemistry, Division of Oral Biological Sciences, Kyushu University, 3-1-1 Maidashi, Higashi-ku, Fukuoka 812-8582, Japan
[b] Section of Orthodontics and Dentofacial Orthopedics, Division of Oral Health, Growth and Development, Kyushu University, 3-1-1 Maidashi, Higashi-ku, Fukuoka 812-8582, Japan
[c] Laboratory of Oral Pathology, Division of Maxillofacial Diagnostic and Surgical Sciences, Kyushu University, 3-1-1 Maidashi, Higashi-ku, Fukuoka 812-8582, Japan
[d] Division of Physiology, Kyushu Dental University, 2-6-1 Manazuru, Kokurakita-ku, Kitakyushu 803-8580, Japan
[e] Department of Human, Information and Life Sciences, School of Health Sciences, University of Occupational and Environmental Health, 1-1 Iseigaoka, Yahatanishi-ku, Kitakyushu 807-8555, Japan
[f] Division of Anatomy and Cell Biology of the Hard Tissue, Department of Tissue Regeneration and Reconstruction, Niigata University Graduate School of Medical and Dental Sciences, 2-5274 Gakkocho-dori, Chuo-ku, Niigata 951-8514, Japan
[g] Department of Physiological Sciences and Molecular Biology, Fukuoka Dental College, 2-5-1 Tamura, Sawara-ku, Fukuoka 814-0175, Japan
[h] Oral Medicine Center, Fukuoka Dental College, 2-5-1 Tamura, Sawara-ku, Fukuoka 814-0175, Japan
[i] Section of Bioengineering, Fukuoka Dental College, 2-5-1 Tamura, Sawara-ku, Fukuoka 814-0175, Japan
[j] Department of Rehabilitation, Yugawara Hospital, Japan Community Health Care Organization, 2-21-6 Chuo, Yugawara, Ashigara-shimo, Kanagawa 259-0396, Japan
[k] Field of Human Disease Models, Major in Advanced Life Sciences and Medicine, Institute of Laboratory Animals, Tokyo Women's Medical University, 8-1 Kawada-cho, Shinjuku-ku, Tokyo 162-8666, Japan
[l] Oral Health/Brain Health/Total Health Research Center, Faculty of Dental Science, Kyushu University, 3-1-1 Maidashi, Higashi-ku, Fukuoka 812-8582, Japan

ARTICLE INFO

Keywords:
Crk-associated substrate protein
Ameloblasts
Dental enamel
Biomineralizaion
Cell polarity

ABSTRACT

Amelogenesis consists of secretory, transition, maturation, and post-maturation stages, and the morphological changes of ameloblasts at each stage are closely related to their function. p130 Crk-associated substrate (Cas) is a scaffold protein that modulates essential cellular processes, including cell adhesion, cytoskeletal changes, and polarization. The expression of p130Cas was observed from the secretory stage to the maturation stage in ameloblasts. Epithelial cell-specific p130Cas-deficient ($p130Cas^{\Delta epi-}$) mice exhibited enamel hypomineralization with chalk-like white mandibular incisors in young mice and attrition in aged mouse molars. A micro-computed tomography analysis and Vickers micro-hardness testing showed thinner enamel, lower enamel mineral density and hardness in $p130Cas^{\Delta epi-}$ mice in comparison to $p130Cas^{flox/flox}$ mice. Scanning electron microscopy, and an energy dispersive X-ray spectroscopy analysis indicated the disturbance of the enamel rod structure and lower Ca and P contents in $p130Cas^{\Delta epi-}$ mice, respectively. The disorganized arrangement of ameloblasts, especially in the maturation stage, was observed in $p130Cas^{\Delta epi-}$ mice. Furthermore, expression levels of enamel matrix proteins, such as amelogenin and ameloblastin in the secretory stage, and functional markers, such as alkaline phosphatase and iron accumulation, and $Na^+/Ca^{2+}+K^+$-exchanger in the maturation stage were reduced in $p130Cas^{\Delta epi-}$ mice. These findings suggest that p130Cas plays important roles in amelogenesis (197 words).

Abbreviations: Cas, Crk-associated substrate; KRT, cytokeratin; μCT, micro-computed tomography; SEM, scanning electron microscopy; NCKX, $Na^+/Ca^{2+}+K^+$-exchanger.

* Corresponding author at: Oral Health/Brain Health/Total Health Research Center, Faculty of Dental Science, Kyushu University, 3-1-1 Maidashi, Higashi-ku, Fukuoka 812-8582, Japan.
E-mail address: ejimi@dent.kyushu-u.ac.jp (E. Jimi).

https://doi.org/10.1016/j.bone.2021.116210
Received 24 July 2021; Received in revised form 17 September 2021; Accepted 18 September 2021
Available online 28 September 2021

1. Introduction

Enamel is the hardest and most highly mineralized tissue in the body. Mature enamel is composed of regular hexagonal hydroxyapatite (HA) ($Ca_{10}[PO_4]_6[OH]_2$) crystals and is characterized by containing almost no matrix protein. Enamel consists of a highly organized structure of interwoven prisms and inter-prismatic material, which are both made up of HA crystals [1].

Unlike other hard tissues, such as dentin and bone derived from mesenchyme, enamel is formed by ameloblasts derived from the dental epithelium [2]. The differentiation of dental epithelial cells into functional ameloblasts involves of multiple steps, including proliferation, secretory, transition, maturation, and post-maturation stages, which are accompanied by morphological and functional changes. During the proliferation stage, short columnar inner enamel epithelial cells (IEEs) actively proliferate and then, IEEs grow into columnar cells (pre-ameloblasts) with more protein-synthesizing organelles. In the secretory stage, ameloblasts grow and polarize, forming conical processes called Tomes' processes, which deposit enamel in the form of rods. Enamel matrix proteins, such as amelogenin, enamelin, and ameloblastin, are secreted during this period. After the enamel reaches full thickness during the transition stage, the height of the ameloblasts decreases and the protein synthesis organelles significantly decrease during the transition stage. In the maturation stage, ameloblasts regulate and transport specific ions required for the deposition of minerals, while degrading enamel matrix proteins and resorbing the degraded proteins and water. Ameloblasts initiate a series of repetitive morphological changes on the surface of the enamel, with distal tight junctions and deep membrane folds appearing periodically (ruffled-ended ameloblasts), then disappearing for short intervals (smooth-ended ameloblast). In the post-maturation stage, ameloblasts become short cuboidal cells. Particularly important in these steps are the secretory stage, in which the enamel matrix proteins are produced, and the maturation stage, in which mineralization progresses. The presence of these two functional stages is a major feature of amelogenesis [1–3].

Amelogenesis imperfecta (AI) is a disease in which different genes cause abnormal enamel formation in all or some teeth [1]. Its phenotype is diverse and complex; however, it can be divided into hypoplastic, hypomaturation, and hypocalcified types based on the quality and quantity of the affected enamel. The hypoplastic type is caused by some abnormalities during the substrate formation stage, and the enamel calcification is almost the same as that of the normal type; however, it is thin. The low-maturity form is due to inadequate degradation of enamel matrix protein, and the enamel thickness is similar to normal, while calcification is poor. Hypocalcification is sometimes classified as a hypomineralization type together with a low maturity type, and is caused by less Ca^{2+} supply [1].

Since the discovery that the mutations in the AMELX gene, which encodes amelogenin, an enamel matrix protein, were responsible for AI [4], mutations and dysfunctions in many genes have been reported to cause AI [1]. Furthermore, enamel hypoplasia, like AI in humans, has been observed in mouse models, indicating that various genes play an important role in amelogenesis [1]. For example, mutations in Distal-less homeobox 3 (*DLX3*) are known to cause autosomal dominantly-inherited trichodentoosseous syndrome and AI hypomaturation-hypoplastic type with taurodontism [5,6]. Mutations or deletion of genes including *AMBN*, and *ENAM*, encoding enamel matrix proteins, ameloblastin [7–9], and enamelin [10–12], respectively, and *MMP20* [1,13,14], and *KLK4* [1,15,16], encoding enamel matrix proteases, are also observed in AI patients and mouse models. Mutations in the genes, *AMTN* [17–19] and *FAM83H* [20–22], which are important for the interaction between ameloblasts and extracellular matrix, were found in AI patients, and each gene-deficient mice showed enamel hypoplasia. Furthermore, hypomaturation AI was observed due to gene mutations or deficiency of *WDR72* [1,23,24] and *SLC24A4*, which encode NCKX4 [25–28], which is an important transporter for protein and ions. Therefore, recent increases in our understanding of the gene variations that cause AI provide new information about the various cellular and extracellular biological functions that are essential for amelogenesis.

p130 Crk-associated substrate (Cas) belongs to the Cas protein family and acts an adapter protein. It is involved in signal transduction from cell surface receptors including integrin, to the intracellular molecules and even nuclei through association with various proteins [29,30]. p130Cas plays critical roles in various cellular functions, including cell adhesion, spreading, migration, invasion, proliferation, and mechanosensing of the surrounding physical environment [29,30]. Osteoclasts are multinucleated giant cells that differentiate from monocyte/macrophage lineage cells and resorb bone. Resorbing osteoclasts adhere to the bone surface to form a tight sealing at the bone surface and secrete H^+ and Cl^- to decalcify minerals, and proteolytic enzymes, such as cathepsin K and matrix metalloprotease 9 (MMP9) to degrade the bone matrix under a raffled border [31,32]. We previously reported that osteoclast-specific p130Cas conditional knockout mice showed osteopetrosis because osteoclasts failed to resorb bone due to the lack of a ruffled border, suggesting that p130Cas plays an important role in the osteoclastic bone resorption of osteoclasts [33]. Ameloblasts similar to osteoclasts form the ruffled-end, and secrete enamel proteins, and their degrading enzymes. Therefore, we hypothesize that p130Cas is also involved in ameloblast differentiation and function.

In this study, we clarify the presence of p130Cas and its physiological roles in ameloblasts by analyzing epithelial cell-specific p130Cas-deficient mice.

2. Materials and methods

2.1. Generation of epithelial cell-specific p130Cas-deficient mice

Knockout mice lacking the epithelial cell specific p130Cas gene ($p130Cas^{\Delta epi-}$) were generated by closing cytokeratin 14 (*KRT14*)-*Cre* transgenic mice (Jackson Laboratory) with floxed-p130Cas mice (B6;129P2-p130Cas, tmHomy>) [33]. $p130Cas^{flox/flox}$ littermates were used as controls. The handling of the mice and all procedures were approved by the Animal Care Committee of Kyushu University, according to the guidelines of the Japanese Council on Animal Care (Approval Number: A20-138-2).

2.2. Radiological assessment

The internal structure of each sample was observed by micro-computed tomography (μ-CT) (Skyscan 1075 KHS; Kontich, Belgium) using an X-ray voltage of 50 kV, a 0.5 mm aluminum filter, and a pixel size of 9 μm. Then each sample was reconstructed and analyzed using CTAn software program (version 1.18.8, Bruker, Kontich, Belgium). To determine the degree of enamel mineral density (EMD), hemimandibles from $p130Cas^{flox/flox}$ and $p130Cas^{\Delta epi-}$ mice were scanned at a pixel size of 9 μm using μ-CT (Skyscan 1075). A standard curve of 5 hydroxyapatite standards of known density was used for a quantitative analysis. The most incisal slice containing the most mineralized enamel was identified visually. Measurements were made at 500-μm intervals (50 slices at a 10-μm interval) and slices from three mice per group at the same developmental stage were averaged using the CTAn software program.

2.3. SEM and EDX analysis

The mandibular incisors of $p130Cas^{flox/flox}$ and $p130Cas^{\Delta epi-}$ mice aged 6 weeks were dissected and fixed with 2.5% glutaraldehyde, 2% paraformaldehyde, 0.1 M phosphate buffer (pH 7.4). The surface morphology of each sample was observed using a scanning electron microscope (SEM: S-3400 N; Hitachi High Technologies Co., Tokyo, Japan) under an accelerating voltage of 10 kV. Coating of the sample with a gold-palladium alloy was performed by magnetron sputtering

(MSP-1 s; Vacuum Device, Ibaraki, Japan). Element mapping at the microstructural level was carried out using an energy dispersive X-ray (EDX) spectrometry system (Quantax70, Bruker, Kanagawa, Japan).

2.4. Vickers micro-hardness testing

The left mandibles were dissected from *p130Cas*$^{flox/flox}$ and *p130Cas*$^{\Delta epi-}$ mice (age: 6 weeks), washed, and dehydrated with graded ethanol. The samples, which were kept moist at all times, were fixed by composite resin on the metal plate, and sagittally ground (Handimet 2 Roll Grinder, Buehler, Lake Bluff, IL, USA) and automatically lapped (ml-160a, Maruto Instrument Co., Ltd., Tokyo, Japan). The mandibular incisor enamel micro-hardness was measured at 5 different sites of the incisors per mouse in 3 mice per group using a Vickers micro-hardness tester (MXT50, Matsuzawa, Co., Ltd., Akita, Japan) under a 100-g load for 10 s.

2.5. Histological analysis

Mandibles were fixed with 4% paraformaldehyde and decalcified with Osteosoft (Merck, Darmstadt, Germany). Sagittal paraffin sections (4 μm thick) were cut. Sections were analyzed with hematoxylin and eosin (H&E) staining. To evaluate the iron transport ability, sections were stained with Berlin blue. For the immunohistochemical analysis, sections were stained with antibodies specific for p130Cas (#38560; Abcam Inc., Cambridge, UK), bone-specific alkaline phosphatase (ALP) (#M190; Takara Bio. Inc., Shiga, Japan), amelogenin (#pc-062; Kamiya Biomedical Company, Seattle, WA, USA), ameloblastin (#sc-271,912, Santa Cruz Biotechnology, Santa Cruz, CA, USA), or $Na^+/Ca^{2+}+K^+$-exchanger (NCKX4) (#18992-AP, Proteintech Group Inc., Rosemont, IL, USA). The primary antibodies were visualized using a horseradish peroxidase (HRP)-conjugated anti-rabbit secondary antibody (Nichirei Bio., Tokyo, Japan) and a DAB Peroxidase (HRP) Substrate Kit (Vector laboratories, CA, USA). Negative controls were prepared by substituting PBS for each primary antibody as a negative immunohistochemical staining control. Sections were analyzed using a IXplore Pro microscope (Olympus, Tokyo, Japan).

2.6. Statistical analysis

All data are shown as the mean ± standard deviation (SD). Comparisons of the means between two groups were carried out using an unpaired Student's *t*-test using Microsoft Excel 2019 (Reymond, WA, USA). *P* values of <0.05 were considered to indicate statistical significance.

3. Results

3.1. The expression of p130Cas during amelogenesis

We previously generated osteoclast-specific p130Cas-deficient mice and reported that their osteoclasts unable to form a ruffled border and showed the impairment of bone resorption [33]. Since it is known that ameloblasts in the maturation stage form a ruffled-end [1–3], we hypothesized that ameloblasts express p130Cas and that the molecule might play an important role also in enamel formation. Since murine incisors grow continuously and thus provide an experimental advantage (as all developmental stages of amelogenesis can be examined in a sagittal section) [34], we confirmed the expression of p130Cas in the ameloblasts immunohistochemically using mandibular incisors. The expression of p130Cas was not observed in dental epithelial cells or mesenchymal cells of the cervical loop (Fig. 1A), but its expression was observed from the apical end to the incisal edge, especially from the secretory stage to the maturation stage, during ameloblast differentiation (Fig. 1B–E). Specimens were stained without primary antibody and then counterstained with hematoxylin to detect nuclei as negative control (Fig. 1F).

3.2. The incisors of epithelial cell-specific p130Cas-deficient (*p130Cas*$^{\Delta epi-}$) mice showed lower mineralization

Since p130Cas deficiency shows embryonic lethality in mice [35], we generated epithelial cell-specific p130Cas-deficient (*p130Cas*$^{flox/flox}$*KRT14*$^{Cre/+}$: *p130Cas*$^{\Delta epi-}$) mice by crossing *p130Cas*$^{flox/flox}$ with *KRT14* $^{Cre/+}$ mice to address the role of p130Cas in tooth development *in*

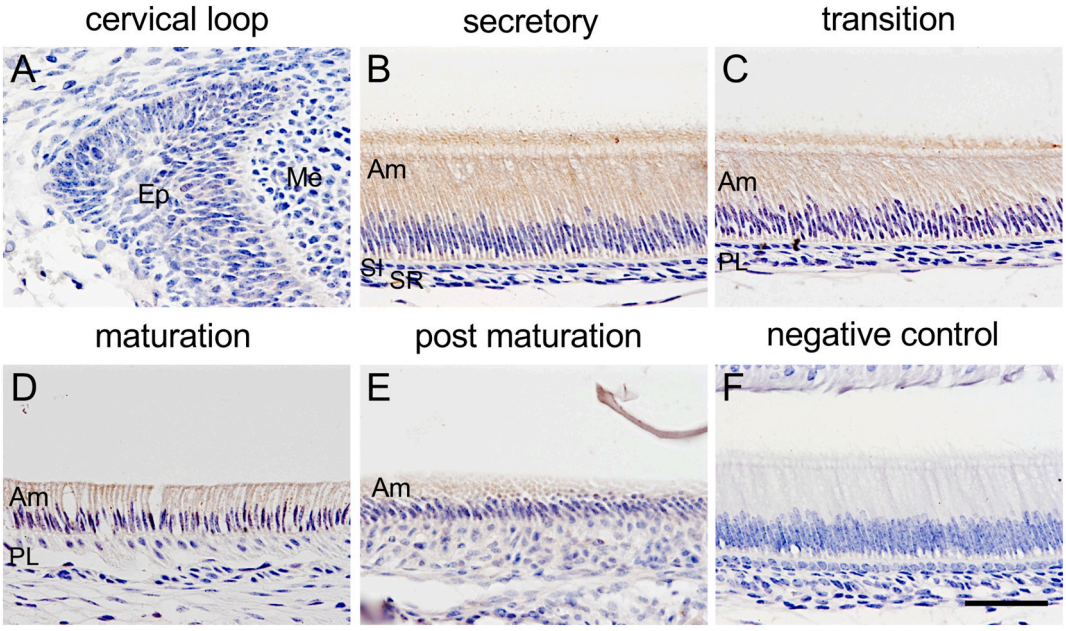

Fig. 1. The expression of p130Cas during amelogenesis. Immunohistochemical analysis of p130Cas in mandibular incisors of 2-week-old male wild-type mice. Sagittal paraffin sections prepared from mandibular incisors of 2-week-old male wild-type mice ($n = 5$ mice per group, 15 slides per group) were stained with antibodies against p130Cas (panels A–E) or without the primary antibody (panel F). The sections were counterstained with hematoxylin. Ep: epithelial cells, Me: mesenchymal cells, Am: ameloblasts, SI: stratum intermedium, SR: stellate reticulum, PL: papillary layer. Scale bar: 50 μm.

vivo. The body weight and growth rate of *p130Cas*$^{\Delta epi-}$ mice did not show any significant differences compared to those of *p130Cas*$^{flox/flox}$ mice (data not shown). The immunohistochemical analysis of mandibular incisors of 2-week-old mice revealed that the expression of p130Cas was detected in both ameloblasts (secretory stage) and odontoblasts of *p130Cas*$^{flox/flox}$ mice (Fig. 2A, panel a). The expression of p130Cas was observed in odontoblasts but not ameloblasts of *p130Cas*$^{\Delta epi-}$ mice (Fig. 2A, panel b). No signals were detected without the primary antibody (Fig. 2A, panel c). These results indicated that p130Cas was selectively deleted in the ameloblasts. Although there were no obvious abnormalities in the number, the appearance, and the morphology of teeth in *p130Cas*$^{\Delta epi-}$ mice, the color of the mandibular incisors was white and opaque (Fig. 2B). The maxillary incisors of 6-week-old male *p130Cas*$^{\Delta epi-}$ mice varied from pale yellow (Fig. 2B, panel b, 11 out of 19 mice, 57.9%) to yellow (Fig. 2B, panel c, 8 out of 19 mice, 42.1%), which was not much different from *p130Cas*$^{flox/flox}$ mice (Fig. 2B, panel a). Thus, we extracted the maxillary incisors, and then measured the length of the yellow-colored part, and calculated the ratio of the length of the yellow-colored part to the total length. The total length of the extracted maxillary incisors did not change, but the length of the yellow-colored part was shorter in the *p130Cas*$^{\Delta epi-}$ mice, and the ratio of the length of the yellow-colored part to the total length was also lower in the *p130Cas*$^{\Delta epi-}$ mice (Fig. 2C, D). The yellow coloration of the maxillary incisors became darker with age, and there was no significant difference in appearance after 20 weeks of age. However, as in the 6-week-old *p130Cas*$^{\Delta epi-}$ mice, the length of the yellow-colored part and the ratio of the length of the yellow-colored part per total length of the extracted maxillary incisor in the female 12-month-old *p130Cas*$^{\Delta epi-}$ mice were shorter in comparison to age-matched *p130Cas*$^{flox/flox}$ mice (Supplemental Fig. 1A, B). The yellow coloration of the mouse incisors means that the teeth contained iron, indicating the degree of enamel maturity. There was not much difference in the erupted part, but when the tooth was extracted and observed, there was a difference in the length of the yellow-colored part in the maxilla, suggesting that there were abnormalities, such as delay in enamel maturation of the incisors of the *p130Cas*$^{\Delta epi-}$ mice.

Three-dimensional (3D) image reconstruction revealed that *p130Cas*$^{\Delta epi-}$ mice exhibited no obvious differences in tooth eruption, development, and occlusion compared with *p130Cas*$^{flox/flox}$ mice (Fig. 3A, left panels). There was no significant difference in the enamel border in the maxillary incisors between *p130Cas*$^{flox/flox}$ mice and *p130Cas*$^{\Delta epi-}$ mice; however, in the mandibular incisors of *p130Cas*$^{\Delta epi-}$ mice, the enamel border was unclear and the enamel surface seemed to be rough (Fig. 3A, right panels). To compare the volume of enamel, the mandibular incisors were sliced from the front. When the mandibular incisor was sliced at eruption area, the enamel thickness of the *p130Cas*$^{\Delta epi-}$ mice was slightly thinner in comparison to *p130Cas*$^{flox/flox}$ mice, but when the mandibular incisor was sliced anterior to the first molar, the enamel was hard to detect in the *p130Cas*$^{\Delta epi-}$ mice, suggesting that enamel mineralization was impaired in *p130Cas*$^{\Delta epi-}$ mice (Fig. 3B). Consistent with these results, the quantitative measurement of the enamel mineral density indicated that the mineral content in the

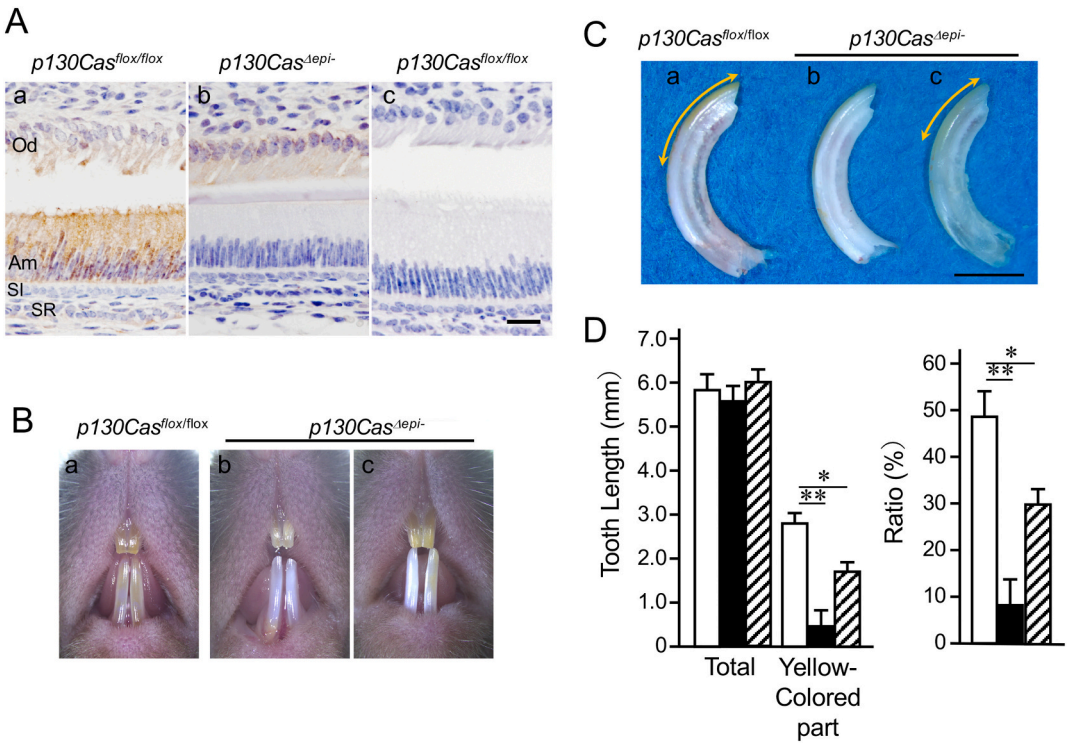

Fig. 2. The tooth phenotype of epithelial cell-specific p130Cas-deficient (p130Cas$^{\Delta epi-}$) mice. (A) Sagittal paraffin sections of secretory-stage mandibular incisors prepared from 2-week-old of *p130Cas*$^{flox/flox}$ (panels a, c) and *p130Cas*$^{\Delta epi-}$ mice (panel b) (n = 5 mice per group, 15 sections per group) were stained with antibodies against p130Cas (panels a, b), or without the primary antibody (panel c). The sections were counterstained with hematoxylin. Am: ameloblasts, Od: odontoblasts, SI: stratum intermedium, SR: stellate reticulum, Scale bar: 20 μm. (B) Incisors of 6-week-old male *p130Cas*$^{flox/flox}$ ($n = 16$ mice) and *p130Cas*$^{\Delta epi-}$ mice ($n = 19$ mice). Mandibular incisors of *p130Cas*$^{\Delta epi-}$ mice were whiter than those of *p130Cas*$^{flox/flox}$ mice. There are two types of maxillary incisors of 6-week-old male *p130Cas*$^{\Delta epi-}$ mice, a pale yellow one (b; $n = 11$ mice) and a yellow one (c; $n = 8$ mice) that was almost the same as the type observed in *p130Cas*$^{flox/flox}$ mice (a; $n = 15$ mice). (C) Maxillary incisors were extracted from 6-week-old male *p130Cas*$^{flox/flox}$ (a; n = 5 mice) and *p130Cas*$^{\Delta epi-}$ mice (b; $n = 6$ mice, c; n = 5 mice). In (C), a, b, and c indicate the right maxillary incisors extracted from mice a, b, and c shown in (B). Scale bar: 2 mm. (D) The total length and length of the yellow-colored parts were measured and the ratio of the length of the yellow-colored parts per total length of the extracted incisors is shown (more than 8 incisors per group). The open column indicates *p130Cas*$^{flox/flox}$ mice. The closed column and hatched column indicate the pale yellow-colored and yellow that was almost the same as that observed in *p130Cas*$^{flox/flox}$ mice, respectively. The data are expressed as the mean ± SD. *, $p < 0.05$, **, $p < 0.01$. (For interpretation of the references to color in this figure legend, the reader is referred to the web version of this article.)

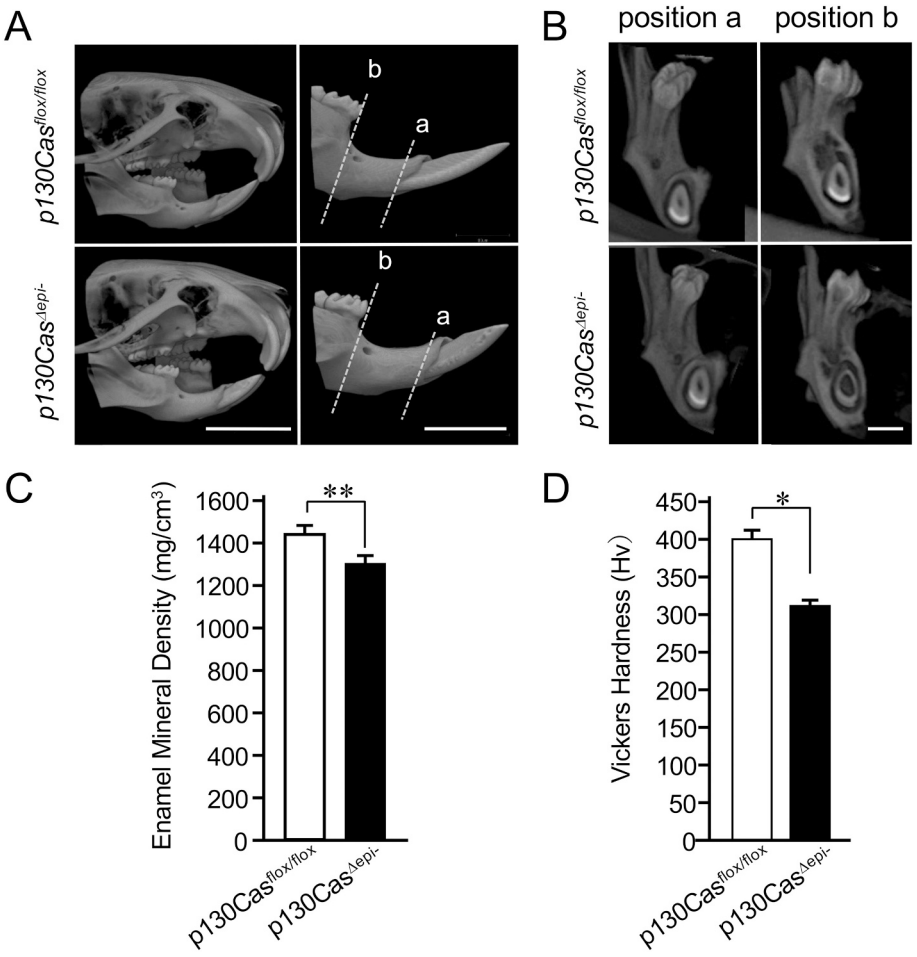

Fig. 3. Incisors of *p130Cas*$^{\Delta epi-}$ mice showed lower mineralization. (A) Three-dimensional reconstruction of μCT scans of the head and incisors of 8-week-old male *p130Cas*$^{flox/flox}$ and *p130Cas*$^{\Delta epi-}$ mice (n = 5) Scale bars: 5 mm (left), 2 mm (right). (B) Three-dimensional reconstruction of μCT scans of mandibular incisors, sliced from the front (positions a and b in Fig. 2A) of 8-week-old male *p130Cas*$^{flox/flox}$ and *p130Cas*$^{\Delta epi-}$ mice (n = 5). Scale bar: 2 mm. (C) A quantitative analysis of the enamel mineral density of right and left mandibular incisors of 6-week-old male *p130Cas*$^{flox/flox}$ (open column, n = 5 mice and 10 different points) and *p130Cas*$^{\Delta epi-}$ mice (closed column, n = 5 mice and 10 different points). (D) A quantitative analysis of the enamel micro-hardness of right and left mandibular incisors of 6-week-old male *p130Cas*$^{flox/flox}$ (open column, *n* = 3 mice and 15 different points) and *p130Cas*$^{\Delta epi-}$ (closed column, n = 3 mice and 15 different points) mice. The data are expressed as the mean ± SD (n = 15). *, $p < 0.05$. **, $p < 0.01$.

enamel was significantly lower in *p130Cas*$^{\Delta epi-}$ mice than that in *p130Cas*$^{flox/flox}$ mice (Fig. 3C). Furthermore, the enamel hardness of the mandibular incisors of *p130Cas*$^{\Delta epi-}$ mice was also lower than that of *p130Cas*$^{flox/flox}$ mice (Fig. 3D).

On the other hand, there was no significant difference in the molar morphology between 6-week-old male *p130Cas*$^{flox/flox}$ mice and *p130Cas*$^{\Delta epi-}$ mice (Supplemental Fig. 1C). However, in the 12-month-old female *p130Cas*$^{\Delta epi-}$ mice, the molar cusps were worn in comparison to those of age-matched *p130Cas*$^{flox/flox}$ mice (Supplemental Fig. 1D).

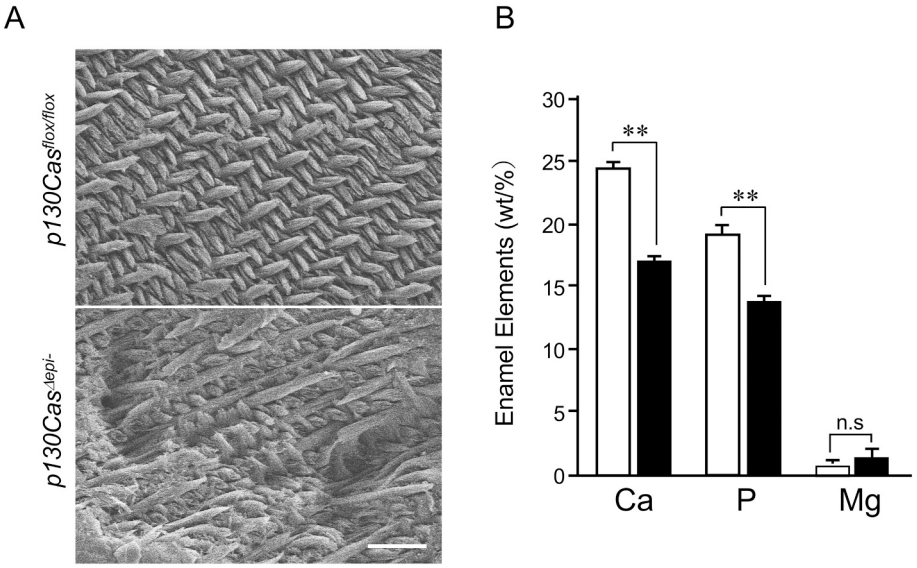

Fig. 4. An abnormal enamel rod structure was observed in *p130Cas*$^{\Delta epi-}$ mice. (A) Scanning electron microscopy (SEM) images showing the enamel from 6-week-old male *p130Cas*$^{flox/flox}$ (n = 6 mice) and *p130Cas*$^{\Delta epi-}$ mice (n = 6 mice). Scale bar: 10 μm. (B) The calcium, phosphorus and magnesium contents in the enamel of right and left mandibular incisors of 6-week-old male *p130Cas*$^{flox/flox}$ (open column, n = 5 mice and 10 different points) and *p130Cas*$^{\Delta ep}$ (closed column, n = 5 mice and 10 different points) mice. The data are expressed as the mean ± SD. *, $p < 0.05$. **, $p < 0.01$, n.s. not significance.

3.3. Abnormal enamel rod structure in $p130Cas^{\Delta epi-}$ mice

We further examined the microstructural transformation in teeth from $p130Cas^{\Delta epi-}$ mice, using scanning electron microscopy (SEM). For acid-etched incisors, a remarkable difference was observed in the structure and organization of enamel rods between $p130Cas^{\Delta epi-}$ mice and $p130Cas^{flox/flox}$ mice (Fig. 4A). The enamel rods of the incisors of $p130Cas^{flox/flox}$ mice were regularly arranged, but the arrangement of the enamel rods of the incisors of $p130Cas^{\Delta epi-}$ mice was totally disturbed (Fig. 4A). Similarly, the structure and organization of enamel rods were also disturbed in the mandibular incisors of 12-month-old female $p130Cas^{\Delta epi-}$ mice in comparison to those of $p130Cas^{flox/flox}$ mice (Supplemental Fig. 1E).

Comparing the arrangement of the enamel rods of the mandibular first molar of the 6-week-old male $p130Cas^{\Delta epi-}$ mice and $p130Cas^{flox/flox}$ mice, the enamel rods of the mandibular first molar of the $p130Cas^{flox/flox}$ mice were regularly arranged. However, the arrangement of the enamel rods of the mandibular first molars of $p130Cas^{\Delta epi-}$ mice was disturbed (Supplemental Fig. 1F). Furthermore, similar disordered arrangement of the enamel rods of the mandibular first molars was also observed in 12-month-old female $p130Cas^{\Delta epi-}$ mice (Supplemental Fig. 1G). These results suggest that the weak enamel caused by the disordered arrangement of the enamel rods found in the molar enamel of 6-week-old $p130Cas^{\Delta epi-}$ became more prominent with attrition over time.

We next measured the trace element content of mandibular incisor, including calcium, phosphorus, and magnesium of enamel using EDX spectroscopy. The ratios of calcium, and phosphorus were decreased in the enamel of $p130Cas^{\Delta epi-}$ mice in comparison to those of $p130Cas^{flox/flox}$ mice (Fig. 4B). These results suggested that the suppression of enamel mineralization was caused by the change in the ratios of trace elements contained in the enamel and by the disordered arrangement of the enamel rods.

3.4. Ablation of p130Cas induces disorganization and hypoplasia of the ameloblasts in $p130Cas^{\Delta epi-}$ mice

We first histologically compared the differentiation process of ameloblasts between $p130Cas^{\Delta epi-}$ mice and $p130Cas^{flox/flox}$ mice. There were no apparent differences in the ameloblasts from secretory stage to transitional stage (Fig. 5A, B, E and F). However, the mature ameloblasts of $p130Cas^{\Delta epi-}$ mice were disordered with keratin-like structure (Fig. 5G), partially defective blistering-like (Fig. 5H), or cyst-like (Fig. 5I), while those of $p130Cas^{flox/flox}$ mice were regularly arranged (Fig. 5C, Supplemental Fig. 2, Table 1). Disordered ameloblasts were observed on 25 of the 30 sections (83.3%), of which 9 had defects (Table 1). There were 5 normal cases. At the post-maturation stage, the ameloblasts were arranged almost normally (Fig. 5J), but a disordered arrangement of the ameloblasts was observed in some sections. (Fig. 5K, Table 1).

Table 1
Variations in phenotype in the maturation or post maturation stages of amelogenesis.

		Genotype	
Stage	Phenotype	$p130Cas^{flox/flox}$	$p130Cas^{epi\Delta/-}$
Maturation	Disorder	0/30	25/30
	Defect	0/30	9/30
Post maturation	Disorder	0/30	6/30

Sagittal paraffin sections of mandibular incisors prepared from 2-week-old male $p130Cas^{flox/flox}$ (n = 15 mice) and $p130Cas^{\Delta epi-}$ mice (n = 15 mice) were stained with hematoxylin and eosin. Thirty sections were randomly selected from the prepared sections and observed under a microscope. The number of sections in which ameloblast disorder or a defect in the maturation stage and ameloblast disorder in the post maturation stage was counted, is shown.

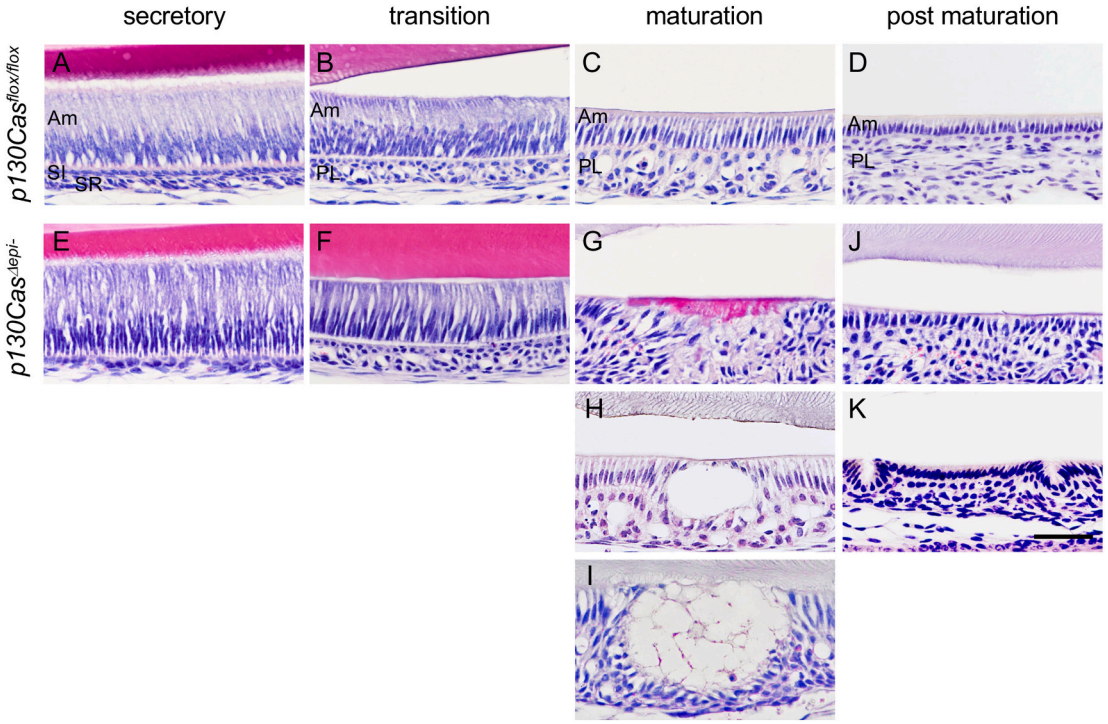

Fig. 5. Ablation of p130Cas induces disorganization of ameloblasts and hypoplasia of the enamel in $p130Cas^{\Delta epi-}$ mice. Sagittal paraffin sections of mandibular incisors prepared from 2-week-old male $p130Cas^{flox/flox}$ (panels A-D) and $p130Cas^{\Delta epi-}$ mice (panels *E*-J), were stained with hematoxylin and eosin (n = 15 mice and 30 sections per group). Am: ameloblasts, SI: stratum intermedium, SR: stellate reticulum, PL: papillary layer. Scale bar: 50 μm.

3.5. Functional abnormalities in ameloblasts of p130Cas$^{\Delta epi-}$ mice

Since the mineralization of enamel in incisors of *p130Cas*$^{\Delta epi-}$ mice was reduced in comparison to *p130Cas*$^{flox/flox}$ mice, we next examined the functional changes in ameloblasts in *p130Cas*$^{\Delta epi-}$ mice. ALP is an enzyme that is highly expressed in the maturation stage of ameloblasts and cells of the stratum intermedium (SI) layer in *p130Cas*$^{flox/flox}$ mice; however, lower expression levels were observed in the ameloblasts in maturation stage with defect of *p130Cas*$^{\Delta epi-}$ mice (Fig. 6, panels c, g). The expression of ALP in the SI layer in the secretory stage of *p130Cas*$^{\Delta epi-}$ mice was comparable to those of *p130Cas*$^{flox/flox}$ mice (Fig. 6A, panels a, e).

Iron pigmentation was detected in ameloblasts and the microvascular structure of the papillary layer at the maturation stage in *p130Cas*$^{flox/flox}$ mice by Berlin blue staining (Fig. 6B). However, iron pigmentation in ameloblasts of maturation stage was almost undetectable in *p130Cas*$^{\Delta epi-}$ mice, suggesting that the iron transport ability was reduced in the ameloblasts of *p130Cas*$^{\Delta epi-}$ mice. These results were consistent with the finding that the incisors of *p130Cas*$^{\Delta epi-}$ mice had a chalk-like white color (Fig. 2B).

3.6. The altered expression of enamel matrix proteins in ameloblasts of p130Cas$^{\Delta epi-}$ mice

To determine whether the hypomaturation of the enamel in *p130Cas*$^{\Delta epi-}$ mice was associated with the expression of enamel matrix proteins, we compared the expression of amelogenin and ameloblastin between *p130Cas*$^{\Delta epi-}$ and *p130Cas*$^{flox/flox}$ mice by immunohistochemistry. The punctate immunoreaction for amelogenin was abundant in the enamel matrix and ameloblasts from secretory stage to maturation stages, and then decreased in the post maturation stage of *p130Cas*$^{flox/flox}$ mice and *p130Cas*$^{\Delta epi-}$ mice (Fig. 7A), but the expression level of amelogenin in the secretory stage of *p130Cas*$^{\Delta epi-}$ mice was particularly less than those of *p130Cas*$^{flox/flox}$ mice (Fig. 7A, a, e). The intense punctate immunoreaction for ameloblastin was found exclusively distal cytoplasm of ameloblasts, throughout all stages of amelogenesis of *p130Cas*$^{flox/flox}$ mice (Fig. 7B, a–d). However, the expression level of ameloblastin was less from secretory to maturation stages *p130Cas*$^{\Delta epi-}$ mice in comparison to those of *p130Cas*$^{flox/flox}$ mice (Fig. 7B).

3.7. The reduced expression of NCKX4 in ameloblasts of p130Cas$^{\Delta epi-}$ mice

Finally, we compared the expression of NCKX4, the mutation of which is known to be a causative gene of amelogenesis imperfecta [25–27], between *p130Cas*$^{\Delta epi-}$ mice and *p130Cas*$^{flox/flox}$ mice. In *p130Cas*$^{flox/flox}$ mice, NCKX4 was expressed in ameloblasts from the secretory stage to the post-maturation stage (Fig. 8, A–D), while the expression level was reduced in ameloblasts of *p130Cas*$^{\Delta epi-}$ mice (Fig. 8, E–H).

4. Discussion

We previously reported that p130Cas has a crucial role in ruffled border formation in osteoclasts, which is necessary for bone resorption [33]. In this study, considering the morphological similarity between osteoclasts with a ruffled border and ameloblasts with a ruffled-end, we examined the role of p130Cas in amelogenesis. We showed that p130Cas was expressed throughout ameloblasts, but that it was particularly strongly expressed from the secretory to the maturation stages. We generated the epithelial cell-specific p130Cas-deficient (*p130Cas*$^{\Delta epi-}$) mice and examined phenotypes in adult mouse incisors. We observed enamel hypomineralization with chalk-like white incisors in *p130Cas*$^{\Delta epi-}$ mice. The maxillary incisors of *p130Cas*$^{\Delta epi-}$ mice were divided into pale yellow-colored parts and parts with the same color as *p130Cas*$^{flox/flox}$ mice. The ratio of the length of yellow-colored part per total length of maxillary incisors of *p130Cas*$^{\Delta epi-}$ mice was shorter than that of the maxillary incisors of *p130Cas*$^{flox/flox}$ mice. Micro-CT and SEM analyses revealed that the enamel hypomineralization was caused by the disordered arrangement of enamel rods and lower Ca and P content in *p130Cas*$^{\Delta epi-}$ mice. Furthermore, a histological analysis showed that the ameloblasts exhibited morphological disorganization; reduced the expression of ALP in the maturation stage, the iron accumulation in the maturation stage, and NCKX4 in the maturation stage in *p130Cas*$^{\Delta epi-}$ mice. In 6-week-old *p130Cas*$^{\Delta epi-}$ mice, there was no significant difference in the morphology or color of the molars; however, the attrition of the molars became more pronounced at old age. Furthermore, structural abnormalities of the enamel rods in the first molar were also observed in both 6-week-old *p130Cas*$^{\Delta epi-}$ mice and aged *p130Cas*$^{\Delta epi-}$ mice. The difference in phenotype between the incisors and molars of *p130Cas*$^{\Delta epi-}$

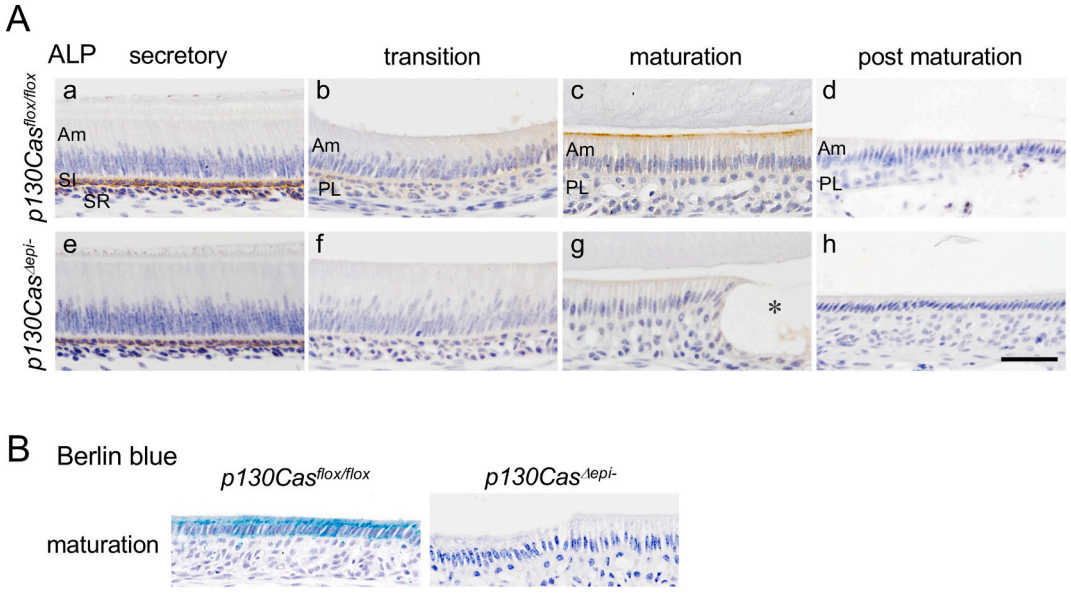

Fig. 6. Functional abnormalities in ameloblasts of p130Cas$^{\Delta epi-}$ mice. Sagittal paraffin sections of mandibular incisors prepared from 2-week-old male *p130Cas*$^{flox/flox}$ (panels a-d) and *p130Cas*$^{\Delta epi-}$ mice (panels e-h), were stained with anti-ALP antibody (n = 5 mice and 15 sections per group) (A) and Berlin blue (B) (n = 5 mice and 15 sections per group). Scale bars: 50 μm. * indicates defect.

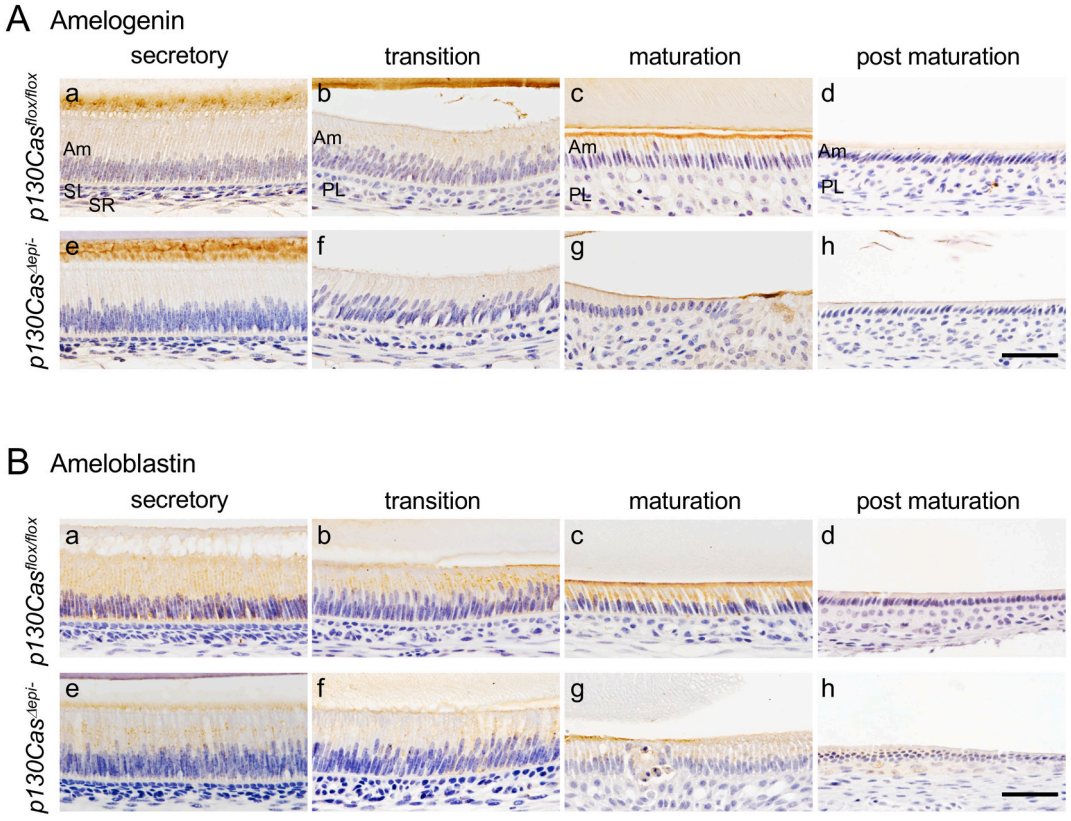

Fig. 7. The altered expression of enamel matrix proteins in ameloblasts of *p130Cas*$^{\Delta epi-}$ mice. Sagittal paraffin sections of mandibular incisors prepared from 2-week-old male *p130Cas*$^{flox/flox}$ (panels a-d) and *p130Cas*$^{\Delta epi-}$ mice (panels e-h), were stained with anti-amelogenin (A) and ameloblastin (B) antibodies ($n = 7$ mice and 20 sections per group). Scale bars: 50 μm.

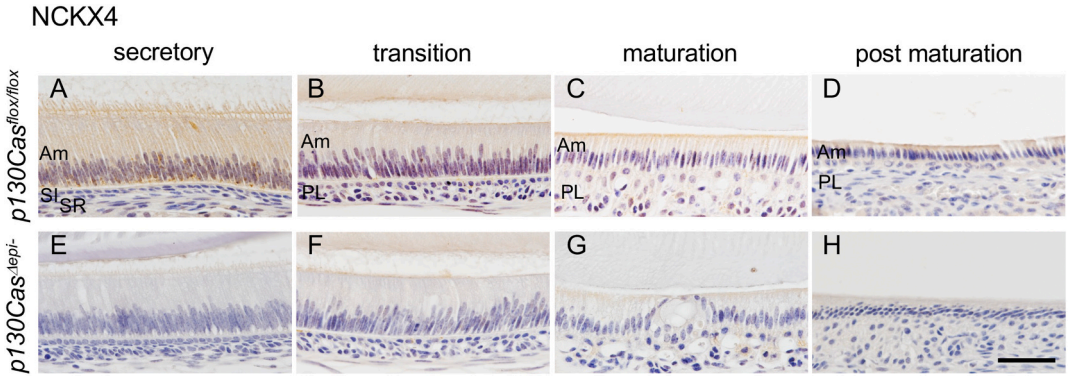

Fig. 8. The reduced expression of NCKX4 in ameloblasts of *p130Cas*$^{\Delta epi-}$ mice. Sagittal paraffin sections of mandibular incisors prepared from 2-week-old male *p130Cas*$^{flox/flox}$ (panels A-D) and *p130Cas*$^{\Delta epi-}$ mice (panels E-H), were stained with anti-NCKX4 antibody (n = 7, mice and 20 sections per group). Scale bar: 50 μm.

mice may be due to the constant growth of mouse incisors. Thus, these results indicate that p130Cas is required for normal amelogenesis.

The morphological defects in ameloblasts in *p130Cas*$^{\Delta epi-}$ mice were mainly observed in the maturation stage. Disordered arrangement of ameloblasts was also observed during the post-maturation stage in approximately 20% of the sections that were observed in detail (6 of 30 cases); however, the frequency was considerably lower than that during the maturation stage. Therefore, the mechanism through which p130Cas maintains these morphologies only during a specific differentiation period is unclear. It has been reported that ameloblast disordered and odontogenic cyst formation cause enamel hypomineralization in *Msx2*-deficient mice [34] and autosomal-recessive mutation, *whitish chalk-like teeth* (*wct*) rats [36]. In *p130Cas*$^{\Delta epi-}$ mice, blistering-like or cyst-like structures were observed in mature ameloblasts, but the frequency was about 30%, which was observed in some mature ameloblasts, and were different from the widespread cysts observed in the transition to premature stages in ameloblasts of *Msx2*-deficient mice or *wct* rats. We examined genetically modified mice in which disorder or defects of ameloblasts were observed during the maturation period; however, few similar phenotypes in mice have been reported thus far.

How p130Cas regulates ameloblast morphology is an interesting subject. Rho guanosine triphosphatase (GTPase) organizes the actin cytoskeleton by cycling between the active GTP-bound and inactive guanosine diphosphate (GDP)-bound forms [37]. RhoA proteins are expressed during ameloblast differentiation, whereas Rho inhibitor and Rho GDI are decreased [38]. Mice expressing the dominant-negative form of RhoA (T19N) under the control of the amelogenin promoter showed enamel hypoplasia and surface defects in the molar cusps by

suppressing ameloblast proliferation and the expression of amelogenin [39]. Another Rho family member, Cdc42 is expressed uniformly distributed during the proliferation and maturation stages. Epithelial cell-specific Cdc42-deficient mice also showed tooth hypomaturation and irregular arrangement of their enamel rods structure, which was likely due to altered ameloblast morphology and the secretion of enamel matrix proteins and proteases [40]. We have previously reported that Rac1, one of Rho protein family, is involved in the formation of ruffled border in osteoclasts as a downstream molecule of p130Cas [33]. Rac1 is also expressed during ameloblast differentiation, but is strongly expressed in polarizing ameloblasts. Epithelial cell-specific Rac1-deficient mice showed enamel hypomineralization with a thin enamel layer [41]. There were shorter ameloblasts in which Tomes' processes of secretory ameloblasts did not develop. Furthermore, the expression of enamel matrix proteins, such as amelogenin and ameloblastin was reduced in Rac1-deficient mice [41]. Because the phenotype in *p130Cas*$^{\Delta epi-}$ mice overlaps with deficient mice of the Rho family protein, it is possible that p130Cas, a downstream molecule of integrin signaling, also regulates the function of Rho family proteins in ameloblasts. Since morphological changes are mainly observed in cells at the maturation stage of amelogenesis, a comprehensive analysis using techniques such as microdissection is required to identify the target molecule of p130Cas.

In *p130Cas*$^{\Delta epi-}$ mice, ameloblasts exhibited morphological disorganization with a reduction of functional markers, such as ALP and iron accumulation. Since ALP is a critical enzyme for the mineralization of tooth and bone, a lack of ALP causes defects in enamel in mice [42–44]. Human patients with hypophosphatasia also show incomplete bone and/or tooth calcification [45]. Although, we have not been able to elucidate the mechanism by which p130Cas regulates the expression of ALP in this study, we have previously reported that TGFβ signaling partially activates p130Cas [46]. Machiya et al. reported that the ALP expression in ameloblasts was suppressed in Smad4-deficient mice, which are TGFβ signaling molecules [47]. Enamel hypoplasia has also been reported in epithelial-specific TGFβ-deficient mice. Taken together, these results suggest that TGF-β regulates the expression of ALP *via* p130Cas-Smad4 during enamel formation [48]. In addition, the color of rodent enamel is yellow, because rodent ameloblasts produce the iron-binding protein, ferritin. Iron transport ability has been reported to be involved in enamel calcification, and iron deposition indicates enamel strength [49,50]. The reduction of ALP and iron accumulation in *p130Cas*$^{\Delta epi-}$ mice indicates defective enamel mineralization. These data obtained from the histological analysis, are consistent with the data from the μCT and SEM analyses.

Enamel matrix proteins are composed of amelogenin, which accounts for up to 90%, enamelin, ameloblastin, and tuftelin [51]. Loss-of-function mutations in these proteins in humans and the deletion of these proteins in mice result in enamel hypoplasia [4,52,53]. Amelogenin-deficient mice exhibited a similar phenotype to human X-linked amelogenesis imperfecta, in which ameloblast differentiation was normal but irregular enamel crystal and thinner enamel were observed [52]. Ameloblastin-deficient mice lack the formation of a true enamel layer and instead only show the deposition of a thin layer of calcified hypoplasia in their dentin [9]. Enamelin-deficient mice do not develop a true enamel layer [12]. Enamel hypomineralization was observed in both Cdc42- and Rac1-deficient mice [40,41]. As with Rac1-deficient mice, the decreased expression of enamel matrix proteins was also observed in *p130Cas*$^{\Delta epi-}$ mice; however, conversely, these enamel matrix proteins were increased in Cdc42-deficient mice. Mice with a point mutation (*Amelx*$^{X/Y64H}$) in the tri-tyrosyl region of the mouse *Amelx* gene showed severe enamel hypomineralization [54]. The enamel micro-structure in *Amelx*$^{X/Y64H}$ mice showed a prismatic structure, which is less ordered and more spaced between the prisms than those of wild-type mice. Although the reason was not mentioned in this study, the arrangement of ameloblasts after the secretory stage was significantly disturbed and a blistering-like structure was observed, but in the post-maturation stage, the ameloblasts regained their normal cuboidal morphology [54]. These results indicate that the production and degradation of enamel matrix protein at the appropriate period for ameloblast differentiation is important for enamel calcification.

During the maturation stage, the active transport of mineral ions into the enamel space needs to be increased to support crystallite growth. Therefore, the efficient and effective transport of cellular cargo is essential for enamel formation [1]. Solute Carrier Family 24, Member 4 (NCKX4) is a member of a family of potassium-dependent sodium/calcium exchangers. NCKX4 is bidirectional electrogenic transporter that regulates Ca^{2+} transport in and out of cells, dependent on the transmembrane ion gradient [55]. The expression of NCKX4 in ameloblasts is most dominant at the apical poles and at the lateral membranes proximal to the apical ends [56]. Mutations in *SLC24A4* genes indicate autosomal recessive amelogenesis imperfecta and enamel hypomineralization is observed [25–27]. NCKX4-deficient mice showed a severe defect of enamel mineralization that reflects impaired amelogenesis [28]. The expression of NCKX4 was decreased in mature ameloblasts of *p130Cas*$^{\Delta epi-}$ mice in comparison to *p130Cas*$^{flox/flox}$ mice, which is considered to be one of the causes of decreased enamel hypomineralization.

A recent study investigated the phenotype of epithelial cell-specific p130Cas-deficient mice (*p130Cas*$^{\Delta epi-}$ mice) using *KRT14-Cre* mice [57]. Three-day-old *p130Cas*$^{\Delta epi-}$ mice showed obvious epidermal thickening due to an imbalance between keratinocyte proliferation and differentiation through the decreased expression of p63 and dysregulated YAP localization in epithelial cells. Furthermore, epithelial cells reduced cell adhesion to extracellular matrix [57]. However, this report did not mention the tooth phenotype. Thus, our study revealed a novel physiological role of p130Cas in enamel maturation. We have also observed a decrease in the adhesion of enamel epithelial cells to extracellular matrix when knocking down p130Cas in the dental epithelial cell line (data not shown), but no decrease in the adhesion of ameloblasts was observed in the histological analysis of teeth in our *p130Cas*$^{\Delta epi-}$ mice. It is difficult to evaluate the function of p130Cas in ameloblasts using the two-dimensional cultures of epithelial cells alone. It is necessary to establish a new culture system (*e.g.*, three-dimensional organ culture or co-culture with odontoblasts) and to analyze the molecular mechanism by which p130Cas regulates ameloblast differentiation and its function.

In conclusion, our finding showed that deletion of p130Cas in ameloblasts decreased the degree of mineralization and maturation of the incisors and molars. These results indicate a novel physiological role of p130Cas in enamel maturation.

Funding

This study was supported by the research grant for OBT Research Center from the Kyushu University (to E.J.) and by the Japan Society for the Promotion of Science (JSPS) KAKENHI Grant (17K19773 to E.J.).

CRediT authorship contribution statement

Akane Inoue: Investigation, Formal analysis, Writing – original draft, Writing – review & editing. **Tamotsu Kiyoshima:** Supervision, Writing – review & editing. **Keigo Yoshizaki:** Investigation, Writing – review & editing. **Chihiro Nakatomi:** Investigation, Writing – review & editing. **Mitsushiro Nakatomi:** Supervision, Writing – review & editing. **Hayato Ohshima:** Investigation, Supervision, Writing – review & editing. **Masashi Shin:** Investigation, Supervision, Writing – review & editing. **Jing Gao:** Writing – review & editing. **Kanji Tsuru:** Supervision, Writing – review & editing. **Koji Okabe:** Supervision, Writing – review & editing. **Ichiro Nakamura:** Supervision, Writing – review & editing. **Hiroaki Honda:** Resources, Writing – review & editing. **Miho Matsuda:** Writing – review & editing. **Ichiro Takahashi:** Supervision, Writing – review & editing. **Eijiro Jimi:** Funding acquisition,

Conceptualization, Writing – review & editing.

Declaration of competing interest

The authors have declared no conflict of interest.

Acknowledgments

The authors thank Mr. Hiroshi Otowa for his technical assistance in data collection of histology.

Appendix A. Supplementary data

Supplementary data to this article can be found online at https://doi.org/10.1016/j.bone.2021.116210.

References

[1] C.E.L. Smith, J.A. Poulter, A. Antanaviciute, J. Kirkham, S.J. Brookes, C. F. Inglehearn, A.J. Mighell, Amelogenesis imperfecta; genes, proteins, and pathways, Front. Physiol. 435 (8) (2017) 35, https://doi.org/10.3389/fphys.2017.00435.

[2] I. Thesleff, From understanding tooth development to bioengineering of teeth, Eur. J. Oral Sci. 126 (1) (2018) 67–71, https://doi.org/10.1111/eos.12421.

[3] Bei M Molecular genetics of ameloblast cell lineage, J. Exp. Zool. B Mol. Dev. Evol. 312B (5) (2009) 437–444, https://doi.org/10.1002/jez.b.21261.

[4] M. Lagerström, N. Dahl, Y. Nakahori, Y. Nakagome, B. Bäckman, U. Landegren, U. Pettersson, A deletion in the amelogenin gene (AMG) causes X-linked amelogenesis imperfecta (AIH1), Genomics. 10 (4) (1991) 971–975, https://doi.org/10.1016/0888-7543(91)90187-j.

[5] J.R. Lichtenstein, R.W. Warson, Syndrome of dental anomalies, curly hair and sclerotic bones, Birth Defects Orig. Artic. Ser. 7 (7) (1971) 308–311.

[6] J.A. Price, J.T. Wright, K. Kula, D.W. Bowden, T.C. Hart, A common DLX3 gene mutation is responsible for tricho-dento-osseous syndrome in Virginia and North Carolina families, J. Med. Genet. 35 (10) (1998) 825–828, https://doi.org/10.1136/jmg.35.10.825.

[7] J.A. Poulter, G. Murillo, S.J. Brookes, C.E. Smith, D.A. Parry, S. Silva, J. Kirkham, C.F. Inglehearn, A.J. Mighell, Deletion of ameloblastin exon 6 is associated with amelogenesis imperfecta, Hum. Mol. Genet. 23 (20) (2014) 5317–5324, https://doi.org/10.1093/hmg/ddu247 (Epub 2014 May 23).

[8] M.K. Prasad, V. Geoffroy, S. Vicaire, B. Jost, M. Dumas, S. Le Gras, M. Switala, B. Gasse, V. Laugel-Haushalter, M. Paschaki, B. Leheup, D. Droz, A. Dalstein, A. Loing, B. Grollemund, M. Muller-Bolla, S. Lopez-Cazaux, M. Minoux, S. Jung, F. Obry, V. Vogt, J.L. Davideau, T. Davit-Beal, A.S. Kaiser, U. Moog, B. Richard, J. J. Morrier, J.P. Duprez, S. Odent, I. Bailleul-Forestier, M.M. Rousset, L. Merametdijan, A. Toutain, C. Joseph, F. Giuliano, J.C. Dahlet, A. Courval, M. El Alloussi, S. Laouina, S. Soskin, N. Guffon, A. Dieux, B. Doray, S. Feierabend, E. Ginglinger, B. Fournier, M. de la Dure Molla, Y. Alembik, C. Tardieu, F. Clauss, A. Berdal, C. Stoetzel, M.C. Manière, H. Dollfus, A. Bloch-Zupan, A targeted next-generation sequencing assay for the molecular diagnosis of genetic disorders with orodental involvement, J. Med. Genet. 53 (2) (2016) 98–110, https://doi.org/10.1136/jmedgenet-2015-103302.

[9] S. Fukumoto, T. Kiba, B. Hall, N. Iehara, T. Nakamura, G. Longenecker, P. H. Krebsbach, A. Nanci, A.B. Kulkarni, Y. Yamada, Ameloblastin is a cell adhesion molecule required for maintaining the differentiation state of ameloblasts, J. Cell Biol. 167 (5) (2004) 973–983, https://doi.org/10.1083/jcb.200409077.

[10] M.H. Rajpar, K. Harley, C. Laing, R.M. Davies, M.J. Dixon, Mutation of the gene encoding the enamel-specific protein, enamelin, causes autosomal-dominant amelogenesis imperfecta, Hum. Mol. Genet. 10 (16) (2001) 1673–1677, https://doi.org/10.1093/hmg/10.16.1673.

[11] D. Ozdemir, P.S. Hart, E. Firatli, G. Aren, O.H. Ryu, T.C. Hart, Phenotype of ENAM mutations is dosage-dependent, J. Dent. Res. 84 (11) (2005) 1036–1041, https://doi.org/10.1177/154405910508401113.

[12] J.C. Hu, Y. Hu, C.E. Smith, M.D. McKee, J.T. Wright, Y. Yamakoshi, P. Papagerakis, G.K. Hunter, J.Q. Feng, F. Yamakoshi, J.P. Simmer, Enamel defects and ameloblast-specific expression in Enam knock-out/lacz knock-in mice, J. Biol. Chem. 283 (16) (2008) 10858–10871, https://doi.org/10.1074/jbc.M710565200.

[13] J.W. Kim, J.P. Simmer, T.C. Hart, P.S. Hart, M.D. Ramaswami, J.D. Bartlett, J. C. Hu, MMP-20 mutation in autosomal recessive pigmented hypomaturation amelogenesis imperfecta, J. Med. Genet. 42 (3) (2005) 271–275, https://doi.org/10.1136/jmg.2004.024505.

[14] J.J. Caterina, Z. Skobe, J. Shi, Y.L. Ding, J.P. Simmer, H. Birkedal-Hansen, J. D. Bartlett, Enamelysin (matrix metalloproteinase 20)-deficient mice display an amelogenesis imperfecta phenotype, J. Biol. Chem. 277 (5) (2002) 49598–49604, https://doi.org/10.1074/jbc.M209100200.

[15] P.S. Hart, T.C. Hart, M.D. Michalec, O.H. Ryu, D. Simmons, S. Hong, J.T. Wright, Mutation in kallikrein 4 causes autosomal recessive hypomaturation amelogenesis imperfecta, J. Med. Genet. 41 (7) (2004) 545–549, https://doi.org/10.1136/jmg.2003.017657.

[16] J.P. Simmer, Y. Hu, R. Lertlam, Y. Yamakoshi, J.C. Hu, Hypomaturation enamel defects in Klk4 knockout/LacZ knockin mice, J. Biol. Chem. 284 (17) (2009) 19110–19121.

[17] C.E. Smith, G. Murillo, S.J. Brookes, J.A. Poulter, S. Silva, J. Kirkham, C. F. Inglehearn, A.J. Mighell, Deletion of amelotin exons 3-6 is associated with amelogenesis imperfecta, Hum. Mol. Genet. 25 (16) (2016) 3578–3587, https://doi.org/10.1093/hmg/ddw203.

[18] R.S. Lacruz, Y. Nakayama, J. Holcroft, V. Nguyen, E. Somogyi-Ganss, M.L. Snead, S. N. White, M.L. Paine, B. Ganss, Targeted overexpression of amelotin disrupts the microstructure of dental enamel, PLoS One 7 (4) (2012), e35200, https://doi.org/10.1371/journal.pone.0035200.

[19] Y. Nakayama, J. Holcroft, B. Ganss, Enamel hypomineralization and structural defects in amelotin-deficient mice, J. Dent. Res. 94 (5) (2015) 697–705, https://doi.org/10.1177/0022034514566214.

[20] G. Mendoza, T.J. Pemberton, K. Lee, R. Scarel-Caminaga, R. Mehrian-Shai, C. Gonzalez-Quevedo, V. Ninis, J. Hartiala, H. Allayee, M.L. Snead, S.M. Leal, S. R. Line, P.I. Patel, A new locus for autosomal dominant amelogenesis imperfecta on chromosome 8q24.3, Hum. Genet. 120 (5) (2007) 653–662, https://doi.org/10.1007/s00439-006-0246-6.

[21] J.W. Kim, S.K. Lee, Z.H. Lee, J.C. Park, K.E. Lee, M.H. Lee, J.T. Park, B.M. Seo, J. C. Hu, J.P. Simmer, FAM83H mutations in families with autosomal-dominant hypocalcified amelogenesis imperfecta, Am. J. Hum. Genet. 82 (2) (2008) 489–494, https://doi.org/10.1016/j.ajhg.2007.09.020.

[22] Y.S. Kweon, K.E. Lee, J. Ko, J.C. Hu, J.P. Simmer, J.W. Kim, Effects of Fam83h overexpression on enamel and dentine formation, Arch. Oral Biol. 58 (9) (2013) 1148–1154, https://doi.org/10.1016/j.archoralbio.2013.03.001.

[23] W. El-Sayed, D.A. Parry, R.C. Shore, M. Ahmed, H. Jafri, Y. Rashid, S. Al-Bahlani, S. Al Harasi, J. Kirkham, C.F. Inglehearn, A.J. Mighell, Mutations in the beta propeller WDR72 cause autosomal-recessive hypomaturation amelogenesis imperfecta, Am. J. Hum. Genet. 85 (5) (2009) 699–705, https://doi.org/10.1016/j.ajhg.2009.09.014.

[24] S.K. Wang, Y. Hu, J. Yang, C.E. Smith, S.M. Nunez, A.S. Richardson, S. Pal, A. C. Samann, J.C. Hu, J.P. Simmer, Critical roles for WDR72 in calcium transport and matrix protein removal during enamel maturation, Mol. Genet. Genomic Med. 3 (4) (2015) 302–319, https://doi.org/10.1002/mgg3.143.

[25] A.L. Bronckers, D. Lyaruu, R. Jalali, J.F. Medina, B. Zandieh-Doulabi, P. K. DenBesten, Ameloblast modulation and transport of Cl^-, Na+, and K^+ during amelogenesis, J. Dent. Res. 94 (12) (2015) 1740–1747, https://doi.org/10.1177/0022034515606900.

[26] D.A. Parry, J.A. Poulter, C.V. Logan, S.J. Brookes, H. Jafri, C.H. Ferguson, B. M. Anwari, Y. Rashid, H. Zhao, C.A. Johnson, C.F. Inglehearn, A.J. Mighell, Identification of mutations in SLC24A4, encoding a potassium-dependent sodium/calcium exchanger, as a cause of amelogenesis imperfecta, Am. J. Hum. Genet. 92 (2) (2013) 307–312, https://doi.org/10.1016/j.ajhg.2013.01.003.

[27] S. Wang, M. Choi, A.S. Richardson, B.M. Reid, F. Seymen, M. Yildirim, E. Tuna, K. Gençay, J.P. Simmer, J.C. Hu, STIM1 and SLC24A4 are critical for enamel maturation, J. Dent. Res. 93 (7) (2014) 94S–100S, https://doi.org/10.1177/0022034514527971.

[28] A.B. Stephan, S. Tobochnik, M. Dibattista, C.M. Wall, J. Reisert, H. Zhao, The Na^+/Ca^{2+} exchanger NCKX4 governs termination and adaptation of the mammalian olfactory response, Nat. Neurosci. 15 (1) (2011) 131–137, https://doi.org/10.1038/nn.2943.

[29] H. Matsui, I. Harada, Y. Sawada, Src, p130Cas, and mechanotransduction in cancer cells, Genes Cancer 3 (5–6) (2012) 394–401, https://doi.org/10.1177/1947601912461443.

[30] P. Camacho Leal Mdel, M. Sciortino, G. Tornillo, S. Colombo, P. Defilippi, S. Cabodi, p130Cas/BCAR1 scaffold protein in tissue homeostasis and pathogenesis, Gene 562 (1) (2015) 1–7, https://doi.org/10.1016/j.gene.2015.02.027.

[31] I. Nakamura, N. Takahashi, E. Jimi, N. Udagawa, T. Suda, Regulation of osteoclast function, Mod, Rheumatol. 22 (2) (2012) 167–177, https://doi.org/10.1007/s10165-011-0530-8.

[32] S. Uehara, N. Udagawa, Y. Kobayashi, Non-canonical Wnt signals regulate cytoskeletal remodeling in osteoclasts, cell Mol, Life Sci. 75 (20) (2018) 3683–3692, https://doi.org/10.1007/s00018-018-2881-1.

[33] Y. Nagai, K. Osawa, H. Fukushima, Y. Tamura, K. Aoki, K. Ohya, H. Yasuda, H. Hikiji, M. Takahashi, Y. Seta, S. Seo, M. Kurokawa, S. Kato, H. Honda, I. Nakamura, K. Maki, E. Jimi, p130Cas, Crk-associated substrate, plays important roles in osteoclastic bone resorption, J. Bone Miner. Res. 28 (12) (2013) 2449–2462, https://doi.org/10.1002/jbmr.1936.

[34] M. Nakatomi, H. Ida-Yonemochi, C. Nakatomi, K. Saito, S. Kenmotsu, R.L. Maas, H. Ohshima, Msx2 prevents stratified squamous epithelium formation in the enamel organ, J. Dent. Res. 97 (12) (2018) 1355–1364, https://doi.org/10.1177/0022034518777746.

[35] H. Honda, H. Oda, T. Nakamoto, Z. Honda, R. Sakai, T. Suzuki, T. Saito, K. Nakamura, K. Nakao, T. Ishikawa, M. Katsuki, Y. Yazaki, H. Hirai H, Cardiovascular anomaly, impaired actin bundling and resistance to Src-induced transformation in mice lacking p130Cas, Nat. Genet. 28 (12) (1998) 361–365, https://doi.org/10.1038/1246.

[36] M. Osawa, S. Kenmotsu, T. Masuyama, K. Taniguchi, T. Uchida, C. Saito, H. Ohshima, Rat wct mutation prevents differentiation of maturation-stage ameloblasts resulting in hypo-mineralization in incisor teeth, Histochem. Cell Biol. 128 (3) (2007) 183–193, https://doi.org/10.1007/s00418-007-0297-3.

[37] S.J. Heasman, A.J. Ridley, Mammalian Rho GTPases: new insights into their functions from in vivo studies, Nat. Rev. Mol. Cell Biol. 9 (9) (2008) 690–701, https://doi.org/10.1038/nrm2476.

[38] J. Hatakeyama, S. Fukumoto, T. Nakamura, N. Haruyama, S. SuzukiS, Y. Hatakeyama, L. Shum, C.W. Gibson, Y. Yamada, A.B. Kulkarni, Synergistic roles of amelogenin and ameloblastin, J. Dent. Res. 88 (4) (2009) 318–322, https://doi.org/10.1177/0022034509334749.

[39] H. Xue, Y. Li, E.T. Everett, K. Ryan, L. Peng, R. Porecha, Y. Yan, A.M. Lucchese, M. A. Kuehl, M.K. Pugach, J. Bouchard, C.W. Gibson, Ameloblasts require active RhoA to generate normal dental enamel, Eur. J. Oral Sci. 121 (4) (2013) 293–302, https://doi.org/10.1111/eos.12059.

[40] Z. Tian, X. Lv, M. Zhang, X. Wang, Y. Chen, P. Tang, P. Xu, L. Zhang, B. Wu, L. Zhang, Deletion of epithelial cell-specific Cdc42 leads to enamel hypermaturation in a conditional knockout mouse model, Biochim. Biophys. Acta Mol. basis Dis. 1864 (8) (2018) 2623–2632, https://doi.org/10.1016/j.bbadis.2018.04.015.

[41] Z. Huang, J. Kim, R.S. Lacruz, P. Bringas Jr., M. Glogauer, T.G. Bromage, V. M. Kaartinen, M.L. Snead, Epithelial-specific knockout of the Rac1 gene leads to enamel defects, Eur. J. Oral Sci. 119 1 (1) (2011) 168–176, https://doi.org/10.1111/j.1600-0722.2011.00904.x.

[42] M.D. McKee, M.C. Yadav, B.L. Foster, M.J. Somerman, C. Farquharson, J.L. Millán, Compounded PHOSPHO1/ALPL deficiencies reduce dentin mineralization, J. Dent. Res. 92 (8) (2013) 721–727, https://doi.org/10.1177/0022034513490958.

[43] K.C. Gasque, B.L. Foster, P. Kuss, M.C. Yadav, J. Liu, T. Kiffer-Moreira, A. van Elsas, N. Hatch, M.J. Somerman, J.L. Millán, Tissue-nonspecific alkaline phosphatase deficiency causes abnormal craniofacial bone development in the Alpl(−/−) mouse model of infantile hypophosphatasia, Bone 67 (2014) 81–94, https://doi.org/10.1016/j.bone.2014.06.040.

[44] M.C. Yadav, R.C. de Oliveira, B.L. Foster, H. Fong, E. Cory, S. Narisawa, R.L. Sah, M. Somerman, M.P. Whyte, J.L. Millán, Enzyme replacement prevents enamel defects in hypophosphatasia mice, J. Bone Miner. Res. 27 (8) (2012) 1722–1734, https://doi.org/10.1002/jbmr.1619.

[45] A. Linglart, M. Biosse-Duplan, Hypophosphatasia, Curr. Osteoporos. Rep. 14 (3) (2016) 95–105, https://doi.org/10.1007/s11914-016-0309-0.

[46] T. Yaginuma, J. Gao, K. Nagata, R. Muroya, F. Huang, H. Nagano, S. Chishaki, T. Matsubara, S. Kokabu, K. Matsuo, T. Kiyoshima, I. Yoshioka, E. Jimi, p130Cas induces bone invasion by oral squamous cell carcinoma by regulating tumor epithelial-mesenchymal transition and cell proliferation, Carcinogenesis. 41 (8) (2020) 1038–1048, https://doi.org/10.1093/carcin/bgaa007.

[47] A. Machiya, S. Tsukamoto, S. Ohte, M. Kuratani, N. Suda, Katagiri T, Smad4-dependent transforming growth factor-β family signaling regulates the differentiation of dental epithelial cells in adult mouse incisors. Bone. 137(2020), pp. 115456. doi: https://doi.org/10.1016/j.bone.2020.115456.

[48] W. Song, Y. Wang, Q. Chu, C. Qi, Y. Gao, Y. Gao, L. Xiang, X. Zhenzhen, Y. Gao, Loss of transforming growth factor-β1 in epithelium cells affects enamelformation in mice, Arch. Oral Biol. 96 (2018) 146–154, https://doi.org/10.1016/j.archoralbio.2018.09.003.

[49] T. Yanagawa, K. Itoh, J. Uwayama, Y. Shibata, A. Yamaguchi, T. Sano, T. Ishii, H. Yoshida, M. Yamamoto, Nrf2 deficiency causes tooth decolourization due to iron transport disorder in enamel organ, Genes Cells 9 (7) (2004) 641–651, https://doi.org/10.1111/j.1356-9597.2004.00753.x.

[50] H. Yoshioka, Y. Yoshiko, T. Minamizaki, S. Suzuki, Y. Koma, A. Nobukiyo, Y. Sotomaru, A. Suzuki, M. Itoh, N. Maeda, Incisor enamel formation is impaired in transgenic rats overexpressing the type III NaPi transporter Slc20a1, Calcif. Tissue Int. 89 (3) (2011) 192–202, https://doi.org/10.1007/s00223-011-9506-0.

[51] C.E. Smith, Cellular and chemical events during enamel maturation, Crit. Rev. Oral Biol. Med. 9 (2) (1998) 128–161, https://doi.org/10.1177/10454411980090020101.

[52] C.W. Gibson, Z.A. Yuan, B. Hall, G. Longenecker, E. Chen, T. Thyagarajan, T. Sreenath, J.T. Wright, S. Decker, R. Piddington, G. Harrison, A.B. Kulkarni, Amelogenin-deficient mice display an amelogenesis imperfecta phenotype, J. Biol. Chem. 276 (34) (2001) 31871–31875, https://doi.org/10.1074/jbc.M104624200.

[53] P.S. Hart, T.C. Hart, J.P. Simmer, J.T. Wright, A nomenclature for X-linked amelogenesis imperfecta, Arch. Oral Biol. 47 (4) (2002) 255–260, https://doi.org/10.1016/s0003-9969(02)00005-5.

[54] M.J. Barron, S.J. Brookes, J. Kirkham, R.C. Shore, C. Hunt, A. Mironov, N. J. Kingswell, J. Maycock, C.A. Shuttleworth, M.J. Dixon, A mutation in the mouse Amelx tri-tyrosyl domain results in impaired secretion of amelogenin and phenocopies human X-linked amelogenesis imperfecta, Hum. Mol. Genet. 19 (7) (2010) 1230–1247, https://doi.org/10.1093/hmg/ddq001.

[55] J. Lytton, Na^+/Ca^{2+} exchangers: three mammalian gene families control Ca^{2+} transport, Biochem. J. 406 (3) (2007) 365–382, https://doi.org/10.1042/BJ20070619.

[56] P. Hu, R.S. Lacruz, C.E. Smith, S.M. Smith, I. Kurtz, M.L. Paine, Expression of the sodium/calcium/potassium exchanger, NCKX4, in ameloblasts, Cells Tissues Organs 196 (6) (2012) 501–509, https://doi.org/10.1159/000337493.

[57] M.D.P. Camacho Leal, A. Costamagna, B. Tassone, S. Saoncella, M. Simoni, D. Natalini, A. Dadone, M. Sciortino, E. Turco, P. Defilippi, E. Calautti, S. Cabodi, Conditional ablation of p130Cas/BCAR1 adaptor protein impairs epidermal homeostasis by altering cell adhesion and differentiation, Cell Commun, Signal. 16 (1) (2018) 73, https://doi.org/10.1186/s12964-018-0289-z.